JCTC Journal of Chemical Theory and Computation

ARTICLE

pubs.acs.org/JCTC

Electron Attachment to Diselenides Revisited: Se−Se Bond Cleavage Is Neither Adiabatic nor the Most Favorable Process

José A. Gámez and Manuel Yáñez*

Departamento de Química, Módulo 13, Facultad de Ciencias, Universidad Autónoma de Madrid, Campus de Excelencia UAM-CSIC, Cantoblanco, 28049-Madrid, Spain

ABSTRACT: Up to now it has been generally assumed that the electron capture on diselenides XSeSeX′ produces a fragmentation of the Se−Se bond. However, our high-level ab initio calculations indicate that this is the case only when the substituents X and X′ attached to the diselenide bridge have low electronegativity. Also importantly, even when the two substituents are of similar electronegativity, the Se−Se bond cleavage rarely is an adiabatic process. For low-electronegative X substituents, the extra electron is placed in the σ^*(Se−Se) antibonding orbital, and the cleavage of the Se−Se bond is the most favorable process. However, the mechanism of this bond breaking is more intricate than previously assumed, and for asymmetric derivatives it proceeds through a conical intersection (CI). These findings emphasize the importance of using accurate ab initio calculations, rather than the usually employed density functional theory approaches, when dealing with reactions in biochemistry and organometallic chemistry, because the characterization of a CI requires the use of multireference methods to account for the mixing of states. When X is highly electronegative, the σ^*(Se−X) antibonding orbital becomes highly stabilized with respect to the σ^*(Se−Se) strongly favoring the cleavage of the Se-X bond, whereas the Se−Se remains practically unperturbed. Finally, when comparing the present results on diselenides with those of the disulfide analogues, it is apparent that the activation barriers and the final products of the different unimolecular reactions are higher in energy for the diselenides, in spite of the higher antioxidant strength of diselenides. This seems to indicate that the electron detachment process, less favorable for diselenides than for disulfides, competes with the electron-capture dissociation process and therefore should also be considered to explain the different antioxidant ability of these compounds.

INTRODUCTION

Selenium is an essential trace element which has received an increased interest as it has been identified in a large range of living beings, including humans.[1] It is primarily present in proteins, mainly under the form of the amino acids selenocysteine (Sec) and selenomethionine. Selenoproteins have been reported to play important and diverse roles in organisms, like elimination of peroxides and other oxidant agents, cancer prevention, and inflammation protection.[2−4] Besides, sulfur and selenium share many physicochemical properties, and consequently, selenium usually accompanies or even substitutes sulfur in organisms. Indeed, the mutation of cysteine (Cys) to Sec has been proved to be very conservative, preserving the structure and the biological functionality of the selenomutant.[5−15] Nevertheless, the substitution of Cys by Sec may bring significant advantages as it is the case for some oxireductases containing catalytic redox-active Sec,[16] whose Cys mutants are typically 100−1000 times less active.[17]

Diselenide compounds are of special interest within the huge family of selenium derivatives for their applications in organic synthesis[18−20] and as therapeutic drugs.[21,22] Besides, they are also found in proteins as diselenide bridges,[23] in a similar fashion to sulfur-containing peptides. Diselenides are well-known for their high antioxidant activity,[24−26] which is actually higher than that of disulfides, so the study of their reductive cleavage has attracted considerable attention.[27−30] However, there is not enough information to fully understand the mechanism of this process. In the present contribution we would like to shed some light on this open question by modeling the reductive cleavage of diselenides with the electron-capture dissociation (ECD) reaction, a process largely investigated for disulfides[31−36] but which has not received such attention in the case of diselenides. Previous studies on dimethyldiselenide[37,38] indicate that electron attachment yields mainly the breaking of the Se−Se linkage since the extra electron is accommodated in the σ^*(Se−Se) antibonding orbital, like for disulfides, although these results are not sufficient to get a general picture of the electron-capture process in diselenides.

When an electron is added to a bond A−B, it may happen that the bond is preserved, a two-center, three-electron (2c3e) A∴B bond being established, or that the bond gets broken, the centers being bound by means of charge−dipole interactions. A previous study in our group has shown that both situations are encountered when an extra electron is added to a diselenide depending on the electronegativity of the substituent of the diselenide bond.[39] The distinction about the nature of the activated bonds is of great relevance from the mechanistic point of view. The 2c3e bonds are characterized by a charge fluctuation between the bonding centers, rendering a nearly equal sharing of the unpaired charge.[40] However, as the bond stretches, it may happen that the extra charge and spin density, both initially delocalized throughout the bond, separate and localize into different fragments, a phenomenon known as charge−spin separation. For this reason several authors[41,42] have pointed out that a proper description of the dissociation of 2c3e linkages has to appropriately account for

Received: April 4, 2011
Published: May 13, 2011

a delocalized covalent ground state for the minimum and a localized ionic one for the broken fragments, with the consequent (avoided) crossing of such states at certain bond distances.

The theoretical treatment of several electronic states simultaneously requires the use of special methodology, mainly when they are quite close in energy or even cross. Density functional theory (DFT) is frequently used in biochemistry, but it is inadequate to describe situations of near degeneracy or states crossing. Moreover it is well-known that standard DFT dramatically fails to describe the dissociation of odd-electron bonds.[41−44] This failure is attributed, in part, to the self-interaction error (SIE), an unbalanced description of the exchange and correlation terms in approximate DFT functionals. SIE can be alleviated with a certain amount of HF exchange, i.e., with hybrid functionals,[45] but, since the extent of the SIE varies along the potential energy surface (PES),[43,44] a hybrid functional properly describing a particular region of the PES is likely to fail at other regions, so they do not provide a general solution to the problem. Many SIE-free functionals have been developed following the recipe proposed by Perdew and Zunger,[46] although they are still not well suited to describe the dissociation of 2c3e bonds.[43] Other corrections, like the one proposed by Chermette et al.,[47] show also good results but depend on nuclear charges, which are not physically observable and are difficult to accurately determine.

As DFT provides a troublesome description of the dissociation of odd-electron bonds, wave function methods seem a more reliable alternative. However, previous theoretical studies on the cleavage of diselenides by electron attachment were performed with DFT or other unsuitable methods, and their conclusions may be compromised. Moreover, such works were based on symmetric molecules or systems bearing low-electronegative substituents. These situations are far from reality as proteins are highly asymmetric, and also, they create an environment where diselenides are exposed to substituents with varying electron-withdrawing strength, distorting the electronic density along the bond. The aim of the present contribution is to fully determine how these two factors: the electronegativity of the substituents and the asymmetry of the system influence the ECD reaction of diselenides, as some preliminary results[48] suggest that they do play an important role in the dissociation process. For this purpose, the CH_3SeSeX (X = NH_2, OH, and F) set of molecules has been chosen as representative of asymmetric diselenides with substituents of increasing electronegativity, which can be compared with HSeSeH and $CH_3SeSeCH_3$ to determine the influence of the asymmetry in the Se−Se bond cleavage.

COMPUTATIONAL METHODS

Throughout the Introduction Section we mentioned the inadequacy of standard DFT-based methods to describe the dissociation of odd-electron systems. This failure has been traditionally attributed to the SIE, which has been renamed more recently as delocalization error,[49] present when, due to delocalization, atomic centers bear fractional charges. Both approaches lead to the same behavior: Approximate functionals tend to underestimate the energy of systems with fractional charges. Consequently, MP2 perturbation theory was preferred for geometry optimizations and is able to recover enough electronic correlation at a computational affordable cost for the systems here considered. It is noteworthy, nevertheless, that MP2 can lead to erroneous geometries in the case of asymmetric 2c3e bonds.[50] However, in a previous publication[39] we have checked the MP2 estimates against more accurate methods, like coupled-cluster singles and doubles (CCSD), at predicting the geometries of the systems here considered. In addition to this comparison, it has also been proposed a rule to assess the validity of the MP2 geometries.[50] In all cases, MP2 performs pretty well, showing that it can accurately describe the geometries of the diselenides under study. Once a reliable method is decided, the 6-31++G(d,p) (BS1) expansion has been employed as the basis set, as it is flexible enough to describe the bonding situations we deal with. Since we are describing anions, with an electron placed far from the nuclei, the use of diffuse functions is almost compulsory. The optimized geometries were identified as real minima of the potential energy surface by evaluation of the Hessian matrix. Final energies have been corrected with the CCSD(T) approach, able to recover correlation effects beyond second order, and a more extended basis set, namely aug-cc-pVTZ (BS2). Geometry optimizations and Hessian evaluations with BS1 have been performed with the Gaussian03 suite of programs,[51] while the single point calculations with BS2 at the CCSD(T) level were carried out with the MOLPRO 2009.01 package.[52]

As mentioned above, some of the reactions may involve the crossing of different PESs, what makes mandatory the use of multireference methods, among which the most reliable ones are[53] the multireference configuration interaction (MRCI)[54] or the CASSCF/CASPT2[55] methods. In our study the CASSCF/CASPT2 approach has been chosen because it is less computationally demanding than the MRCI approach and it has been shown to produce reliable results.[53,56] Geometries were optimized, when needed, at the CASSCF level with the atomic natural orbital (ANO) basis set described by Pierloot et al.[57] contracted to Se[5s4p3d]/C,N,O,F[3s2p1d]/H[2s1p] (BS3). With these geometries, high-level energies were obtained with the multireference second-order perturbation CASPT2 method and the aforementioned BS2 expansion. The active space was constructed by distributing 10 electrons (11 in the case of anions) in 8 orbitals (9 for the anions), which showed good results in a similar study involving disulfides.[58] The multireference calculations were performed with the MOLCAS 7.2 package of programs.[59]

Table 1. Se−Se and Se−X Bond Lengths (in Å) for the Neutral (CH_3SeSeX) and Most Stable Radical−Anionic ($[CH_3SeSeX]^-$) Diselenide Derivatives Calculated at the MP2/6-31++G(d,p) Level of Theory[a]

X species	H	CH_3	NH_2	OH	F	
CH_3SeSeX	2.340	2.322	2.331	2.295	2.262	d(Se−Se)
$[CH_3SSX]^-$	2.948	2.929	2.957	2.529	2.428	
CH_3SSX	1.484	1.966	1.847	1.833	1.803	d(Se-X)
$[CH_3SSX]^-$	1.483	1.958	1.905	2.016	2.050	

[a] (for X = H, the system is HSeSeH).

RESULTS AND DISCUSSION

Cleavage of the Se−Se Bond. Previous studies on electron capture of diselenides or their reactions with nucleophiles focused on the breaking of the Se−Se linkage. This cleavage seems quite favorable for X = H, CH_3, and NH_2 considering the geometrical changes triggered upon electron capture (see Table 1), with a remarkable increase of the Se−Se distance, while the rest

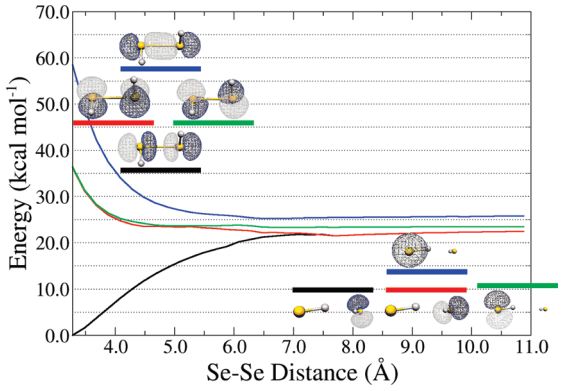

Figure 1. Relative energy (calculated at the CASSCF(11,9)/aug-cc-pVDZ level) of the four lowest states of $[HSeSeH]^-$ with respect to the Se−Se bond distance. To better understand the nature of these states, in the top left corner of the graph the SOMO of each state for d(Se−Se) = 3.280 Å are depicted. In the bottom right corner, the same diagram can be found for d(Se−Se) = 10.680 Å. Note that the upper three excited states can be viewed as core excited states.

of the molecule remains practically unperturbed. However, as the electronegativity of X increases, like for X = OH or F, the activation of the Se−Se bond is less and less important with respect to that of the Se−X linkage, and actually for the anion $[CH_3SeSeF]^-$, the Se···F interaction has greatly lost its covalent character.[39] Based on this, the electron-capture process would yield two different types of fragmentations depending on which of the two linkages Se−Se or Se-X actually cleaves, as a function of the nature of X. Consequently, we will start by studying the Se−Se bond fission in the subset of molecules which seems more prone to it: HSeSeH, $CH_3SeSeCH_3$, and $CH_3SeSeNH_2$.

In the anionic form of these three molecules, the extra electron occupies the σ^*(Se−Se) antibonding orbital being delocalized between both selenium atoms. Therefore, the Se−Se linkage can be viewed as a typical 2c3e bond. As mentioned earlier, the dissociation of the Se−Se bond may involve a crossing between two different states, necessary to connect the reactants, with an unpaired electron delocalized between the two Se atoms, with the products, in which that extra charge will be localized on a particular fragment. However, such a state crossing does not occur for $[HSeSeH]^-$, as shown in Figure 1, which represents the variation of the energy of the four lowest states of $[HSeSeH]^-$ along the Se−Se coordinate.

For the anion in its ground state and in its equilibrium conformation, d(Se−Se) = 3.280 Å, the extra electron occupies the σ^*(Se−Se) orbital. Higher in energy there are two degenerate states whose single occupied molecular orbitals (SOMOs) are π-type linear combinations of the other two p orbitals of selenium. Finally, still higher in energy, there is a fourth state where the extra electron is allocated in the σ(Se−Se) MO. The last three states can be considered as core excited states, since they can be seen as the result of the attachment of the extra electron to an excited state of the neutral system. As shown in Figure 1 they lie very high in energy at the equilibrium distance of the anion, and although they can participate in dissociative electron attachment (DEA) processes when the anion is generated in crossed electron/molecular beams experiments,[60,61] the important point here is that as the Se−Se bond is stretched, these four states come closer in energy until being degenerate at infinity Se−Se distance,

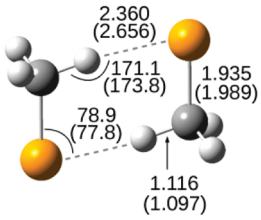

Figure 2. Post-dissociation minimum formed by dissociation of the Se−Se bond in $[CH_3SeSeCH_3]^-$, calculated at the MP2/6-31++G(d,p) (CASSCF/BS3 in parentheses) level of theory. Bond lengths are given in Å and angles, in degrees (°).

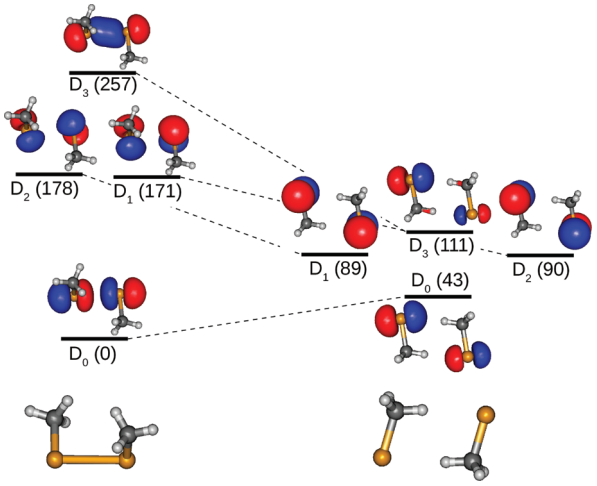

Figure 3. Correlation diagram of the electronic states of the $[CH_3SeSeCH_3]^-$ anion (left-hand side) and the post-dissociation minimum (right-hand side), where each state is represented by its SOMO. The numbers in parentheses correspond to the relative energies (in kJ mol^{-1}) of the states calculated at the MS-CASPT2/aug-cc-pVTZ level.

since each HSe moiety has two symmetry-equivalent p orbitals (four if the two equivalent HSe fragments are considered). We will show in forthcoming sections that when the system is asymmetric, there is indeed a two-state crossing between the ground state and one of the core excited states characterized by a σ(Se−Se) SOMO. For $HSeSeH^-$, as shown on the bottom right corner of Figure 1, already at large Se−Se internuclear distances, the electron is localized either on the right HSe moiety (black and red state) or on the left one (green and blue states), situations which will be strictly equivalent at infinite distance. Consequently, due to the symmetry of the $[HSeSeH]^-$ molecule, the cleavage of the Se−Se bond is a typical adiabatic process. It should be noted that after the Se−Se bond fission a weakly bound complex between the two moieties, $SeX^{\cdot}$ and SeX^-, is formed. This stationary point of the PES will be named hereafter post-dissociation minimum.

A similar situation is found for the also symmetric $[CH_3SeSeCH_3]^-$ anion. In this case a clearer picture can be obtained by using, instead of the potential energy curves of Figure 1, a correlation diagram between the states of the anion in its equilibrium conformation and the states of the post-dissociation minimum (see Figure 2). The description at the MP2 and CASSCF levels of theory of this post-dissociation minimum, where the two $SeCH_3$ moieties are bound together by means of

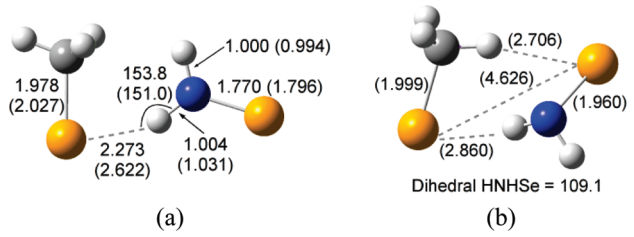

Figure 4. (a) Post-dissociation minimum formed after dissociation and (b) MECP encountered in the Se−Se bond cleavage of the $[CH_3SeSeNH_2]^-$ anion, calculated at the MP2/6-31++G(d,p) (CASSCF/BS3 in parentheses) level of theory. Bond lengths are given in Å and angles, in degrees (°).

two weak C−H···Se interactions, forcing the Se, C, and two H atoms to lie in the same plane in a C_{2h} structure, is rather similar. With this structure, we can now build a correlation diagram between the states of the anion and those of this post-dissociation minimum. An inspection of Figure 3 shows that, as for the HSeSeH system, the Se−Se bond cleavage does not involve the crossing of two different states. Due to the symmetry of the post-dissociation minimum, the extra electron is delocalized between both Se atoms, like in the radical anion. Actually, the structures of the electronic states in both the anion and the post-dissociation minimum are quite similar, although these four states become closer for the post-dissociation minimum, being degenerate at infinite distance like in $[HSeSeH]^-$.

The results obtained for the symmetric HSeSeH and $CH_3SeSeCH_3$ make it interesting to investigate the cleavage of the Se−Se linkage when the symmetry is broken by introducing two substituents with different electronegativity, like in $CH_3SeSeNH_2$. In this case, the most favorable dissociation process leads $[SeCH_3]^- + [SeNH_2]^\cdot$, while the $[SeCH_3]^\cdot + [SeNH_2]^-$ dissociation channel lies 40 kJ mol^{-1} higher in energy. This finding seems to be counterintuitive, since from the electronegativity difference between the methyl and the amino group, one would expect the second dissociation limit to be lower in energy than the first one. However this is not so because the electron affinity (EA) of $[SeCH_3]^\cdot$ is larger than that of $[SeNH_2]^\cdot$. In the former, the lowest unoccupied molecular orbital (LUMO) corresponds to a nonbonding 4p AO of selenium, while for $[SeNH_2]^\cdot$ the LUMO is a π^*(Se−N) MO, arising from a combination between the 4p AO of Se and the lone pair of N, which necessarily rises the energy of the LUMO and, consequently, decreases the EA of the system. The enhanced stability of the $[SeCH_3]^- + [SeNH_2]^\cdot$ products with respect to $[SeCH_3]^\cdot + [SeNH_2]^-$ is also reflected in the structure of the post-dissociation minimum (Figure 4a). Since in the $[SeNH_2]^\cdot$ radical the π^*(Se−N) antibonding is only singly occupied, the Se−N bond retains some double-bond character, and actually the $SeNH_2$ fragment of the post-dissociation minimum (Figure 4a) is planar, the HNH bond angle (115.7°) being close to a pure sp^2 hybridization. Conversely, for the $[SeNH_2]^-$ anion the structure is far form being planar, and the Se−N distance is much longer because the extra electron doubly occupies the π^*(Se−N) antibonding MO. Note that in the post-dissociation minimum both subunits are held together by a Se···HN weak interaction in a way that the $SeNH_2$ fragment is coplanar to the Se and C atoms of the other fragment.

How the extra electron gets localized in the $SeCH_3$ moiety is the question which needs to be answered now because, different

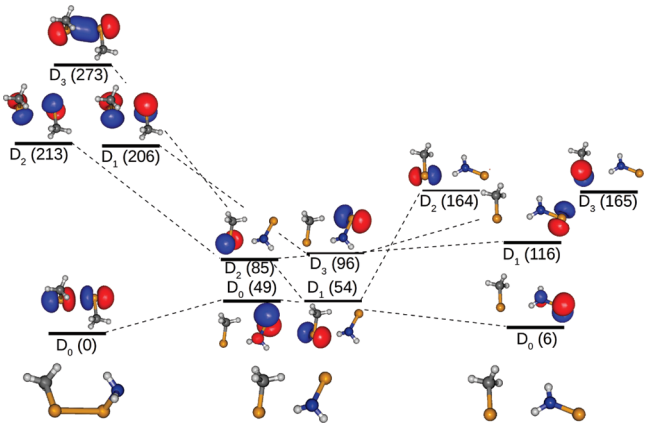

Figure 5. Correlation diagram of the electronic states of the $[CH_3SeSeNH_2]^-$ anion (left-hand side), the post-dissociation minimum (right-hand side), and the MECP (middle part) connecting them. Each state is characterized by its SOMO and its relative energy (in kJ mol^{-1}) in parentheses calculated at the MS-CASPT2/aug-cc-pVTZ level.

from $[HSeSeH]^-$ and $[CH_3SeSeCH_3]^-$, analyzed above, this process cannot be adiabatic. In the $[CH_3SeSeNH_2]^-$ anion in its equilibrium conformation, as in the previous cases, the extra charge is delocalized between both Se, and therefore the charge localization on the $SeCH_3$ moiety can only be accomplished if the σ^*(Se−Se) and σ(Se−Se) MOs strongly interact so that their combination would recover the p orbitals on each selenium, enabling the aforementioned charge localization. Thus, the ground state and one of the core excited states, whose SOMOs are the σ^*(Se−Se) and σ(Se−Se) orbitals, respectively, have to cross. The corresponding minimum-energy crossing point (MECP) structure, which is displayed in Figure 4b, is rather similar to the final post-dissociation minimum since the Se−Se bond is already practically broken, although the nitrogen still exhibits some sp^3 character as suggested by the HNHSe dihedral angle. The localization of this late barrier for the Se−Se bond fission of $[CH_3SeSeNH_2]^-$ contrasts with what has been found for the analogous S−S bond cleavage of the $[CH_3SSNH_2]^-$ anion.[62] For the sulfur derivative, the MECP has a shorter S−S distance and is more similar to that in the equilibrium conformation of the anion. Such an early barrier has been also found for $[CH_3SeSeNH_2]^-$ but about 50 kJ mol^{-1} above the late MECP barrier displayed in Figure 4b.

The correlation diagram between the states of the anion and the post-dissociation minimum connected through the MECP is shown in Figure 5.

The low-lying states for the $[CH_3SeSeNH_2]^-$ anion (left-hand side of the diagram) are similar to those found for $[HSeSeH]^-$ and $[CH_3SeSeCH_3]^-$ anions, i.e., in the ground state the unpaired electron is placed in the σ^*(Se−Se) orbital, higher in energy there are two quasidegenerate states with the p nonbonding orbitals on each Se as SOMOs, while for the highest one the SOMO is the σ (Se−Se) MO. On going to the MECP, the interaction between this latter state (initially D_3) and the ground state (D_0) results in an energy lowering of the former until crossing with the ground state at the MECP. This produces two degenerate states (D_0, D_1) which, on their evolution toward the post-dissociation products, split apart as a consequence of the privileged charge localization on the $SeCH_3$ moiety. Consequently, the two lowest states (D_0, D_1) of the post-dissociation

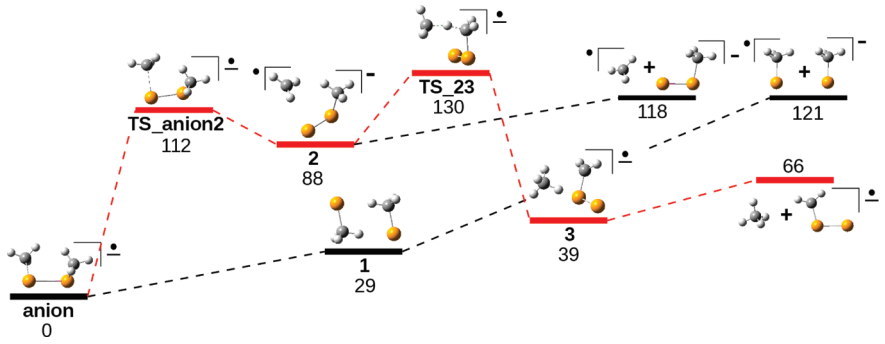

Figure 6. Energy profile associated with the main fragmentations of $[CH_3SeSeCH_3]^-$. The path leading to the loss of CH_4 is highlighted in red. Relative ΔH values (in kJ mol^{-1}) calculated at the CCSD(T)/aug-cc-pVTZ level are displayed under each structure.

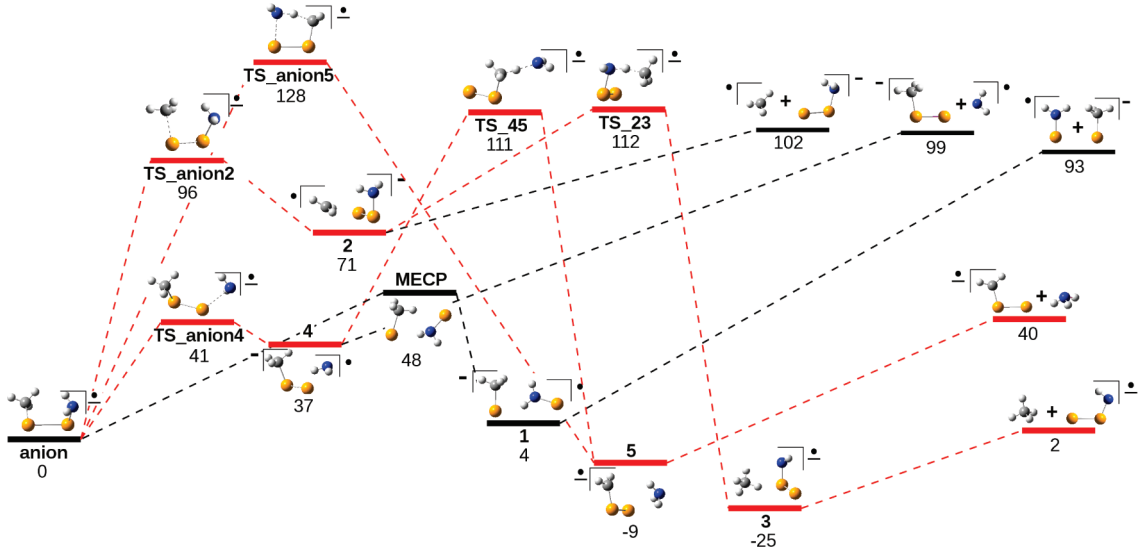

Figure 7. Energy profile associated with the main the main fragmentations of $[CH_3SeSeNH_2]^-$. The paths leading to the loss of CH_4 and NH_3 are highlighted in red. Relative ΔH values (in kJ mol^{-1}) calculated at the CCSD(T)/aug-cc-pVTZ level are displayed under each structure. For the MECP structure, the CASPT2 method was used instead.

minimum localize the unpaired electron at the $SeNH_2$ fragment and the negative charge at the $SeCH_3$ moiety. The fact that these two states are not degenerate reflects the aforementioned resonance between one of these 3p orbitals of selenium and the lone pair of nitrogen in D_0. The most important conclusion is that for strongly asymmetric systems, such as $[CH_3SeSeNH_2]^-$, the cleavage of the Se−Se bond goes necessarily through a conical intersection in order to localize the extra charge on a particular fragment.

Other Fragmentation Products. However, the picture presented in the previous sections for the ECD of diselenides is only a partial one since other fragmentations products are possible. As a matter of fact, for both systems, $[CH_3SeSeCH_3]^-$ and $[CH_3SeSeNH_2]^-$, the most stable fragmentations from the thermodynamic point of view are not the ones discussed so far but the release of neutral molecules: CH_4 and NH_3. To understand why these latter molecules experimentally appear only as secondary products, it is necessary to explore the PES associated with these bond fragmentations (See Figures 6 and 7, respectively).

Both PESs show that, although the release of neutrals is by far the most favorable process from the thermodynamic point of view, due to the significant stability of both CH_4 and NH_3, it has to overcome higher reaction barriers than those associated with the Se−Se bond fission. Besides, the loss of CH_4 and NH_3 is a two-step process (eq 1), which will surely have a negative influence in the rate of the overall reaction.

$$[XH_mSeSeX'H_n]^- \longrightarrow [XH_mSeSe + XH_n]^- \longrightarrow [XH_{m-1}SeSe]^- + X'H_{n+1} \quad (1)$$

As a matter of fact as shown in Figure 6 and 7, in the first step the $[CH_3SeSeX'H_n]^-$ anion leads to a complex between a methyl radical and a $[SeSeX'H_n]^-$ anion (structure **2**), which may dissociate into the two constituents or undergo a hydrogen transfer which would yield CH_4 + $[SeSeX'H_{n-1}]^-$ as final products.

In the case of methyl-amino derivative (X = C, X' = N), a transition structure (**TS_anion5**) connecting directly the anion with complex **5** ($[SeSeCH_2]^{\cdot-}\cdots NH_3$) has been located. Although the corresponding activation barrier is still too high to render the latter fragmentation channel kinetically favorable with respect to the Se−Se bond cleavage, it is noteworthy that a similar transition structure was not found for the fragmentation

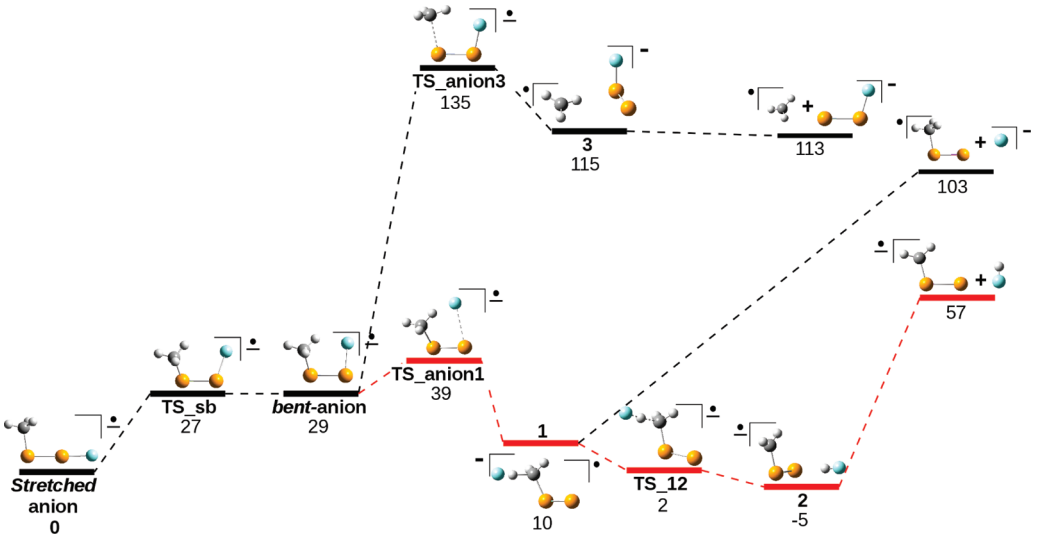

Figure 8. Energy profile associated with the main fragmentations of $[CH_3SeSeF]^-$. The paths leading to the loss of HF is highlighted in red. Relative ΔH values (in kJ mol^{-1}) calculated at the CCSD(T)/aug-cc-pVTZ level are displayed under each structure.

of the $[CH_3SSNH_2]^-$ analogue,[62] and hence, the release of NH_3 would be more probable in the diselenide than in the disulfide. These differences between diselenide and disulfide could be due to the more extended orbitals of selenium, causing the Se−N bonds being longer than the S−N ones favoring the proximity of the NH_2 and the CH_3 groups and therefore the H shift between them. However, for X′ = C, all the efforts to find a similar late-transition structure failed, likely reflecting the lower basicity of the methyl group with respect to that of the amino one.

Preliminary results also suggested that the electronegativity of the substituents has an important influence in the ECD process of diselenides.[48]This effect can be assessed by considering CH_3SeSeF. Recalling the results of Table 1, the electron attachment produces a much larger activation of the Se−F bond than of the Se−Se one, so the $[SeCH_3]^\cdot + [SeF]^-$ dissociation limit lies above in energy than the $[CH_3SeSe]^\cdot + F^-$ one. More importantly, the energy barrier associated to the cleavage of the Se−F bond is quite low (see Figure 8). In particular, the release of HF is the most likely process since the barrier of the Se−F bond fission is of ca. 10 kJ mol^{-1}, and the proton transfer from $[CH_3SeSe]^\cdot$ to F^- is practically barrierless. Actually, although in terms of electronic energies, **TS_12** lies above **1** and **2**, when the zero point energy correction is included, it passes below **1** indicating that in practice the process is barrierless. Regarding the $[CH_3]^\cdot + [SeSeF]^-$ exit channel, which is the third most stable, it is noteworthy that the value of the T_1 diagnosis of the CCSD(T) method (0.03), indicates that the **TS_anion3** has a non-negligible multireference character. When its energy is recalculated with CASPT2, the value obtained (172 kJ mol^{-1}) suggests that this barrier is even higher than shown in Figure 8.

So far, two types of systems have been presented, depending whether the Se−Se or Se−X bond fissions are the most favorable process. The $[CH_3SeSeOH]^-$ radical-anion represents an intermediate situation since the transition states involved in both Se−Se and Se−O bond cleavages, **TS_b3** and **MECP2**, respectively (Figure 9), are of comparable relative energies. It can be observed that this PES is much more intricate than the ones previously discussed. Starting from the most stable anionic isomer, namely stretched-anion, two other isomers can be formed, bent-anion and book-anion,[39] which are better prepared for the breaking of the Se−O and Se−Se linkages, respectively. From the book-anion, the Se−Se bond fission goes through a two-state crossing (**MECP2**), as previously described for $CH_3SeSeNH_2$, to yield structure **6**, where the $[SeCH_3]^-$ and $[SeOH]^\cdot$ moieties are bound together by a Se···HO weak interaction. This intermediate can give rise to two different products: $[SeCH_3]^- + [SeOH]^\cdot$ or $CH_3SeH + [SeO]^-$, which in this case are practically degenerate. The bent-anion can undergo the cleavage of the Se−C bond through the transition structure **TS_b1** to yield structure **1**, which can directly lead to $[CH_3]^\cdot + [SeSeOH]^-$ or $CH_4 + [SeO]^-$ through a hydrogen transfer. More favorable is, nevertheless, the breaking of the Se−O bond to yield structure **3**. This intermediate species can directly lead to $[CH_3SeSe]^- + [OH]^\cdot$ or, more interestingly, undergo an internal charge transfer through **MECP1** to end up in **4**, which is similar to **3** but with an inverse charge polarization. Structure **4** is better prepared to yield, the final products $[CH_2SeSe]^- + H_2O$, through a proton transfer (**TS_45**). The higher energy of $[CH_3SeSe]^\cdot + [OH]^-$ exit channel with respect to $[CH_3SeSe]^- + [OH]^\cdot$ explains why the rupture of the Se−O bond in (**3**) produces a hydroxyl radical. Consequently, the release of H_2O and $HSeCH_3$, which are among the most stable products, is significantly hindered by the high barrier needed to convert **3** into **4**. Conversely, for the analogous disulfide,[62] $[CH_3SSOH]^-$, the $[CH_3SS]^\cdot + [OH]^-$ exit channel was found to be lower in energy, and accordingly, no charge transfer was needed to obtain H_2O and $HSCH_3$. A similar discrepancy is found between the S and Se derivatives as far as the relative stabilities of the $[CH_3X]^\cdot + [XOH]^-$ and $CH_3XH + [XO]^-$ (X = S, Se) products is concerned. According to the more reliable CCSD(T) estimates both exit channels are equally stable when X = Se, whereas for X = S the latter products are ca. 50 kJ mol^{-1} lower in energy.

Comparison between Diselenides and Disulfides. The full mechanisms of the different unimolecular reactions triggered by electron attachment to diselenides can be used to get some insight into the redox strength of sulfur- and selenium-containing proteins. Although sulfur and selenium share many physicochemical properties, valence orbitals of Se are more diffuse than

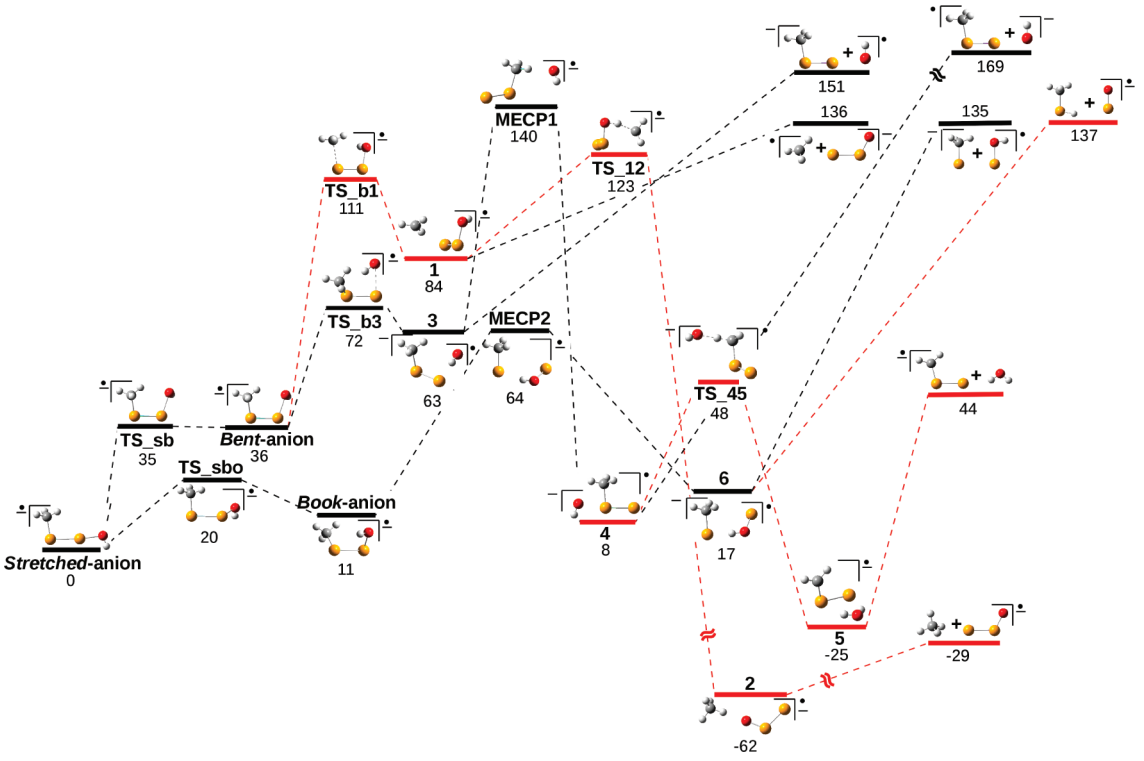

Figure 9. Energy profile associated with the main fragmentations of $[CH_3SeSeOH]^-$. The paths leading to the loss of CH_4 and H_2O are highlighted in red. Relative ΔH values (in kJ mol^{-1}) calculated at the CCSD(T)/aug-cc-pVTZ level are displayed under each structure. For the **MECP1**, **MECP2**, **TS_b3**, and **3** structures, the CASPT2 method was used instead.

those of S, which explains some of the differences between the mechanisms of the ECD of disulfides and diselenides described so far. For instance, the fact that Se−N bonds are larger than S−N ones may rationalize the existence of a direct unimolecular process for the release of NH_3 in $[CH_3SeSeNH_2]^-$, which is absent in $[CH_3SSNH_2]^-$.

More interesting are the differences between $[CH_3SSOH]^-$ and $[CH_3SeSeOH]^-$ regarding the fission of the A−O bond (A = S, Se). As mentioned above, the cleavage of the Se−O linkage produces $[CH_3SeSe]^- + [OH]^{\cdot}$, while for the disulfide $[CH_3SS]^{\cdot} + [OH]^-$ is obtained. This is so because the EA of the $[OH]^{\cdot}$ radical (1.74 eV) is slightly higher than that of $[CH_3SS]^{\cdot}$ (1.72 eV) but significantly lower than that of $[CH_3SeSe]^{\cdot}$ (1.91 eV), likely reflecting a smaller interelectronic repulsion, due to the more diffuse orbitals of Se. The different EA of the $[CH_3SS]^{\cdot}$, $[CH_3SeSe]^{\cdot}$ and $[OH]^{\cdot}$ radicals also helps us to rationalize the different mechanism of the S−O and Se−O bond cleavage. Due to the similar EA of the $[CH_3SS]^{\cdot}$ and $[OH]^{\cdot}$ fragments, the extra electron is nearly delocalized between both moieties (their NBO charges being 0.48 and 0.52 e, respectively), and a conical intersection is needed to accomplish the charge localization after bond breaking, in a similar fashion as in the cleavage of the Se−Se bond previously described. However, the dissimilar EA of the $[CH_3SeSe]^{\cdot}$ and $[OH]^{\cdot}$ produces the extra electron to be more localized on the former (the NBO charges being 0.60 and 0.40 e, respectively), favoring its dissociation into $[CH_3SeSe]^- + [OH]^{\cdot}$ through **TS_b3** (See Figure 9). Although for both $[CH_3SSOH]^-$ and $[CH_3SeSeOH]^-$ the most favorable process from a thermodynamical viewpoint is the release of H_2O (see Figure 9 for the diselenide and Figure 10 of ref 54 for the disulfide), the mechanisms behind are significantly different. In

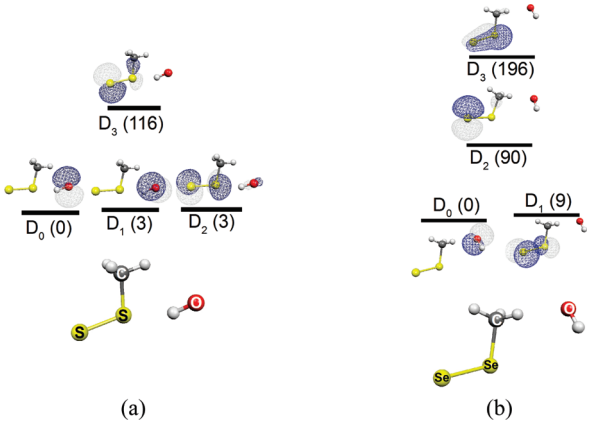

Figure 10. Four lowest states of the MECP structures corresponding to the transition between the $[CH_3AA]^- + [OH]^{\cdot}$ and $[CH_3AA]^{\cdot} + [OH]^-$ products for (a) $[CH_3SSOH]^-$ and (b) $[CH_3SeSeOH]^-$. Each state is characterized by its SOMO and its relative energy (in kJ mol^{-1}) in parentheses calculated at the MS-CASPT2/aug-cc-pVTZ level.

both cases water is formed by a proton transfer from $[CH_3AA]^{\cdot}$ toward $[OH]^-$, but the mechanism by which these two species are formed is different if A = S or Se. While in the case of $[CH_3SSOH]^-$ the breaking of the S−O bond directly leads to $[CH_3SS]^{\cdot} + [OH]^-$, the same process for $[CH_3SeSeOH]^-$ leads to $[CH_3SeSe]^-$ and $[OH]^{\cdot}$, and a subsequent charge transfer to produce $[OH]^-$ through a quite high barrier (**MECP1** of Figure 9) associated with a conical intersection is needed. As a result, the production of water should be much more likely to occur in $[CH_3SSOH]^-$ than in $[CH_3SeSeOH]^-$.

Table 2. Reaction Barriers (B) and Dissociation Energies (DE) of the Cleavage of the A−A and A−X Bonds and the Subsequent Hydrogen-/Proton-Transfer Process (H_{transf}) to Lead to the Loss of Neutrals (CH_4, NH_3, H_2O, and HF) for the CH_3AAXH_n (A = S, Se; X = CH_3, NH_2, OH, F) Systems[a]

barriers / X		B(A−A)	DE(A−A)	B(A−X)	DE(A−X)	H_{transf}	AA + XH_{n+1}	EA
C	S		83[b]	111[b]	80[b]	116[b]	16[b]	23[c]
	Se		121	112	118	130	66	53[d]
N	S	33	35[b]	32[b]	52[b]	78[b]	−20[b]	0[c]
	Se	48	93	41	99	111	40	49[d]
O	S	33	83[b]	56[b]	90[b]	4[b]	−37[b]	11[c]
	Se	64	135	54	151	140	44	73[d]
F	S			21[b]	63[b]	0[b]	23[b]	77[c]
	Se			39	103	0	57	124[d]

[a] The adiabatic EA of the neutral systems is also displayed. All values are in kJ mol^{-1}. [b] Theoretical values taken from ref 62. [c] Theoretical values taken from ref 58. [d] Theoretical values taken from ref 39.

Interestingly, for $[CH_3SSOH]^-$ is its dissociation into $[CH_3SS]^- + [OH]^{\cdot}$ the one that occurs through a CI involving D_0, D_1, and D_2 (See Figure 10), which constitutes the first example of a three state crossing in a thermal reaction occurring in the ground state.[63] These three states correspond to one allocating the unpaired electron in a π^*(S−S) orbital (ground state of $[CH_3SS]^{\cdot}$) and another two where the unpaired electron is in a p orbital of O (the $^2\Pi$ ground state of $[OH]^{\cdot}$) (see Figure 10a). In contrast, for the diselenide analogue the C−H···O interaction, which stabilizes **MECP1**, breaks the degeneracy of the two p orbitals of O (see Figure 10b).

However, the mechanism of the ECD of disulfides and diselenides shows many more differences from a quantitative point of view. As previously mentioned, diselenides are better prepared to accommodate the extra charge due to the more extended orbitals of selenium. Consequently, their unimolecular fragmentations show higher reaction barriers than disulfides, and the final products also lie higher in energy (see Table 2). Experimentally, however, diselenides are stronger reductants than disulfides.[17,64,65] The conciliation between this experimental evidence and the fact that the activation barriers for the unimolecular fragmentation of diselenides are higher than for the disulfide analogues suggests that other processes, such as the ejection of the extra electron, may compete with the ECD. Indeed the EA of these systems (see Table 2) is smaller than the energy required to break the A−A and A−X bonds. This means that a complete picture of the reductive ability of disulfides and diselenides should consider the electron detachment reaction. A first estimate about the extent of this reaction can be obtained from the EA values, which indicate that the electron release process should be less important for diselenides than for disulfides, which would be coherent with the higher reductant strength of the former.

CONCLUSIONS

Based on what has been generally assumed for disulfides and some experimental results on simple diselenides, like dimethyldiselenide, one might expect that the electron capture on diselenides XSeSeX′ produces a fragmentation of the Se−Se bond. However, our results indicate that this is the case only when the substituents X and X′ attached to the diselenide linkage have low electronegativity. Also importantly, even when the two substituents are of similar electronegativity, the Se−Se bond cleavage rarely is an adiabatic process.

In our detailed mechanistic study of the different unimolecular reactions triggered by electron attachment to CH_3SeSeX diselenides, we have found that, quite surprisingly, the most favorable processes, from a thermodynamic point of view, correspond to the release of neutral molecules: CH_4, NH_3, H_2O, and HF. Nevertheless, these products are only likely to be observed for very high electronegative substituents X such as F due to two factors: (i) the occupation of the σ^*(Se−X) antibonding MO by the extra electron is favored when X is a very electronegative element, facilitating the breaking of the Se−X bond and (ii) the activation barrier associated to the proton transfer which produces HF is rather low. Although both conditions (i) and (ii) are fulfilled for X = O, the release of H_2O is disfavored because the breaking of the Se−O bond produces a hydroxyl radical (**3**), which has to undergo an internal charge transfer through a very high conical intersection barrier to obtain a precursor (**4**) with the proper charge distribution to produce $[CH_2SeSe]^{\cdot -} + H_2O$.

For low-electronegative X substituents, the extra electron is placed in the σ^*(Se−Se) antibonding orbital, and the cleavage of the Se−Se bond is the most favorable process. However, the mechanism of this bond breaking is more intricate than previously assumed since, although for symmetric systems, such as HSeSeH or $CH_3SeSeCH_3$, it is strictly adiabatic, for the asymmetric $CH_3SeSeNH_2$ it proceeds through a CI. This crossing between two states is necessary to localize in one of the two fragment products the extra electron, which in the anion is delocalized in the σ^*(Se−Se) antibonding MO. These findings emphasize the importance of using accurate ab initio calculations for the study of electron attachment dissociations of diselenides and, perhaps, other related processes. Many reactions in biochemistry and organometallic chemistry are usually investigated by DFT-based methods due to the size of the systems. However, the characterization of a CI requires the use of multireference methods to account for the mixing of states. This methodological problem has recently been addressed by Shaik and co-workers[66] in the study of the active site of enzymes cytochromes P450 and chloroperoxidase, where the use of CASPT2/MM calculations might change the multistate reactivity of these systems by including some states not present in the DFT/MM picture.

When X is highly electronegative, the σ^*(Se-X) antibonding orbital becomes highly stabilized with respect to the σ^*(Se−Se) strongly favoring the cleavage of the Se−X bond.

Finally, when comparing the present results on diselenides with those of the disulfide analogues, it is apparent that the activation barriers and the final products of the different

unimolecular reactions are higher in energy for the diselenides, in spite of their higher antioxidant strength. This seems to indicate that the electron detachment process, less favorable for diselenides than for disulfides, competes with the ECD process and therefore should also be considered. However, a more detailed study of the electron detachment process needs to be carried out to validate this hypothesis.

AUTHOR INFORMATION

Corresponding Author

*E-mail: manuel.yanez@uam.es.

ACKNOWLEDGMENT

This work has been partially supported by the DGI Project NO CTQ2006-08558/BQU, Project MADRIDSOLAR2, ref.: P2009/PPQ-1533 of the Comunidad Autónoma de Madrid, by Consolider on Molecular Nanoscience CSC2007-00010 and by the COST Action COST CM0702. A generous allocation of computer time at the CCC of the UAM is also acknowledged. J.A.G. acknowledges a contract from the Comunidad Autónoma de Madrid.

REFERENCES

(1) Castellano, S.; Lobanov, A. V.; Chapple, C.; Novoselov, S. V.; Albercht, M.; Hua, D.; Lesc7ure, A.; Lengauer, T.; Krol, A.; Gladyshev, V. N.; Guigo, R. *Proc. Nat. Acad. Sci. U.S.A.* **2005**, *102*, 16188.

(2) Rayman, M. P. *Lancet* **2000**, *356*, 233.

(3) Chen, J.; Berry, M. J. *J. Neurochem.* **2003**, *86*, 1.

(4) Schomburg, L.; Schweizer, U.; Koehrle, J. *Cell. Mol. Life Sci.* **2004**, *61*, 1988.

(5) Frank, W. *Z. Physiol. Chem.* **1964**, *339*, 222.

(6) Walter, R.; du Vigneaud, V. *J. Am. Chem. Soc.* **1965**, *87*, 4192.

(7) Walter, R.; du Vigneaud, V. *J. Am. Chem. Soc.* **1966**, *88*, 1331.

(8) Hartrodt, B.; Neubert, K.; Bierwolf, B.; Blech, W.; Jakubke, H. D. *Tetrahedron Lett.* **1980**, *21*, 2393.

(9) Besse, D.; Budisa, N.; Karnbrock, W.; Minks, C.; Musiol, H. J.; Pegararo, S.; Siedler, F.; Weyher, E.; Moroder, L. *J. Biol. Chem.* **1997**, *378*, 211.

(10) Koider, T.; Itoh, H.; Otaka, A.; Furuya, M.; Kitajima, Y.; Fujii, N. *Chem. Pharm. Bull.* **1993**, *46*, 5382.

(11) Rajarathnam, K.; Sykes, B. D.; Dewald, B.; Baggiolini, M.; Clark-Lewis, I. *Biochemistry* **1999**, *38*, 7653.

(12) Metanis, N.; Keinan, E.; Dawson, P. E. *J. Am. Chem. Soc.* **2006**, *128*, 16684.

(13) Armishaw, C. J.; Daly, N. T.; Adams, D. J.; Craik, D. J.; Alewook, P. F. *J. Biol. Chem.* **2006**, *281*, 14136.

(14) Fori, S.; Pegararo, S.; Rudolph-Böhner, S.; Cramer, J.; Moroder, L. *Biopolymers* **2000**, *53*, 550.

(15) Hondal, R. J.; Nilsson, B. L.; Raines, R. T. *J. Am. Chem. Soc.* **2001**, *123*, 5140.

(16) Jacob, C.; Giles, G. I.; Giles, N. M.; Sies, H. *Angew. Chem., Int. Ed.* **2003**, *42*, 4742.

(17) Johansson, I.; Gafvelin, G.; Amér, E. S. *Biochim. Biophys. Acta* **2005**, *1726*, 1.

(18) Sheu, C.; Sobkowiak, A.; Zhang, L.; Ozbalik, N.; Barton, D. H. R.; Sawyer, D. T. *J. Am. Chem. Soc.* **1989**, *111*, 8030.

(19) Tian, F.; Yu, Z.; Lu, S. *J. Org. Chem.* **2004**, *69*, 4520.

(20) Degrand, C.; Nour, M. *J. Electroanal. Chem.* **1984**, *190*, 213.

(21) Barbosa, N. B. V.; Rocha, J. B. T.; Wondracek, D. C.; Pettroni, J.; Zeni, G.; Nogueira, C. W. *Chem.-Biol. Interact.* **2006**, *3*, 230.

(22) de Freitas, A. S.; Funck, V. R.; Rotta, M. d. S.; Bohrer, D.; Mörschbächer, V.; Puntel, R. L.; Nogueira, C. W.; Farina, M.; Aschner, M.; Rocha, J. B. T. *Brain Res. Bull.* **2009**, *79*, 77.

(23) Shchedrina, V. A.; Novoselov, S. V. *Proc. Nat. Acad. Sci. U.S.A.* **2007**, *104*, 13919.

(24) Arteel, G. E.; Sies, H. *Environ. Toxicol. Pharmacol.* **2001**, *10*, 153.

(25) Meotti, F. C.; Stangherlin, E. C.; Zeni, G.; Nogueira, C. W.; Rocha, J. B. T. *Environ. Res.* **2004**, *94*, 276.

(26) Kumar, B. S.; Kunwar, A.; Ahmad, A.; Kumbhare, L. B.; Jain, V. K.; Priyadarsini, K. I. *Radiat. Environ. Biophys.* **2009**, *48*, 379.

(27) Pearson, J. K.; Boyd, R. J. *J. Phys. Chem. A* **2007**, *111*, 3152.

(28) Movassagh, B.; Shamsipoor, M.; Joshaghani, M. *J. Chem. Res.* **2004**, 148.

(29) Russavskaya, N. V.; Levanova, E. P.; Sukhomazova, E. N.; Grabel'nykh, V. A.; Klyba, L. V.; Zhanchipova, E. R.; Albanov, A. I.; Korchervin, N. A. *Russ. J. Gen. Chem.* **2006**, *76*, 229.

(30) Zhang, S. L.; Tian, F. S. *J. Chem. Res.* **2001**, 198.

(31) Uggerund, E. *Int. J. Mass Spectrom.* **2004**, *234*, 45.

(32) Antonello, S.; Daasbjerg, K.; Jensen, H.; Taddei, F.; Maran, F. *J. Am. Chem. Soc.* **2003**, *125*, 14905.

(33) Sobczyk, M.; Simons, J. *Int. J. Mass Spectrom.* **2006**, *253*, 274.

(34) Anusiewicz, I.; Berdys-Kochanska, J.; Simons, J. *J. Phys. Chem. A* **2005**, *109*, 5801.

(35) Modelli, A.; Jones, D. *J. Phys. Chem. A* **2006**, *110*, 13195.

(36) Yamaji, M.; Tojo, S.; Takehira, K.; Tobita, S.; Fujitsuka, M.; Majima, T. *J. Phys. Chem. A* **2006**, *110*, 13487.

(37) Meija, J.; Beck, T. L.; Caruso, J. A. *J. Am. Soc. Mass Spectrom.* **2004**, *15*, 1325.

(38) Modelli, A.; Jones, D.; Distefano, G.; Tronc, M. *Chem. Phys. Lett.* **1991**, *181*, 361.

(39) Gámez, J. A.; Yáñez, M. *J. Chem. Theory Comput.* **2010**, *6*, 3102.

(40) Hiberty, P. C.; Humbel, S.; Archirel, P. *J. Phys. Chem. A* **1994**, *98*, 11697.

(41) Bally, T.; Sastry, G. N. *J. Phys. Chem. A* **1997**, *101*, 7923.

(42) Chermette, H.; Ciofini, I.; Mariotti, F.; Daul, C. *J. Chem. Phys.* **2001**, *114*, 1447.

(43) Gräfenstein, J.; Kraka, E.; Cremer, D. *Phys. Chem. Chem. Phys.* **2004**, *6*, 1096.

(44) Gräfenstein, J.; Kraka, E.; Cremer, D. *J. Chem. Phys.* **2004**, *120*, 524.

(45) Braïda, B.; Hiberty, P. C.; Savin, A. *J. Phys. Chem. A* **1998**, *102*, 7872.

(46) Perdew, J. P.; Zunger, A. *Phys. Rev. B* **1984**, *23*, 5048.

(47) Chermette, H.; Ciofini, I.; Mariotti, F.; Daul, C. *J. Chem. Phys.* **2001**, *115*, 11068.

(48) Gámez, J. A.; Yáñez, M. *Chem. Commun.* **2011**, *47*, 3939.

(49) Cohen, A.; Mori-Sánchez, P.; Yang, W. *Science* **2008**, *321*, 792.

(50) Braïda, B.; Hiberty, P. C. *J. Phys. Chem. A* **2000**, *104*, 4618.

(51) Frisch, M. J.; Trucks, G. W.; Schlegel, H. B.; Scuseria, G. E.; Robb, M. A.; Cheeseman, J. R.; Montgomery, J. A., Jr. ; Vreven, T.; Kudin, K. N.; Burant, J. C.; Millam, J. M.; Iyengar, S. S.; Tomasi, J.; Barone, V.; Mennucci, B.; Cossi, M.; Scalmani, G.; Rega, N.; Petersson, G. A.; Nakatsuji, H.; Hada, M.; Ehara, M.; Toyota, K.; Fukuda, R.; Hasegawa, J.; Ishida, M.; Nakajima, T.; Honda, Y.; Kitao, O.; Nakai, H.; Klene, M.; Li, X.; Knox, J. E.; Hratchian, H. P.; Cross, J. B.; Bakken, V.; Adamo, C.; Jaramillo, J.; Gomperts, R.; Stratmann, R. E.; Yazyev, O.; Austin, A. J.; Cammi, R.; Pomelli, C.; Ochterski, J. W.; Ayala, P. Y.; Morokuma, K.; Voth, G. A.; Salvador, P.; Dannenberg, J. J.; Zakrzewski, V. G.; Dapprich, S.; Daniels, A. D.; Strain, M. C.; Farkas, O.; Malick, D. K.; Rabuck, A. D.; Raghavachari, K.; Foresman, J. B.; Ortiz, J. V.; Cui, Q.; Baboul, A. G.; Clifford, S.; Cioslowski, J.; Stefanov, B. B.; Liu, G.; Liashenko, A.; Piskorz, P.; Komaromi, I.; Martin, R. L.; Fox, D. J.; Keith, T.; Al-Laham, M. A.; Peng, C. Y.; Nanayakkara, A.; Challacombe, M.; Gill, P. M. W.; Johnson, B.; Chen, W.; Wong, M. W.; Gonzalez, C.; Pople, J. A. *Gaussian* Gaussian Inc., Wallingford, CT, 2004.

(52) Werner, H.-J.; Knowles, P. J.; Lindh, R.; Manby, F. R.; Schütz, M.; Celani, P.; Korona, T.; Mitrushenkov, A.; Rauhut, G.; Adler, T. B.; Amos, R. D.; Bernhardsson, A.; Berning, A.; Cooper, D. L.; Deegan, M. J. O.; Dobbyn, A. J.; Eckert, F.; Goll, E.; Hampel, C.; Hetzer, G.; Hrenar, T.; Knizia, G.; Köppl, C.; Liu, Y.; Lloyd, A. W.; Mata, R. A.; May,

A. J.; McNicholas, S. J.; Meyer, W.; Mura, M. E.; Nicklass, A.; Palmieri, P.; Pflüger, K.; Pitzer, R.; Reiher, M.; Schumann, U.; Stoll, H.; Stone, A. J.; Tarroni, R.; Thorsteinsson, T.; Wang, M.; Wolf, A. *MOLPRO 2009.01*; University College Cardiff Consultants Limited: Cardiff, U.K., 2009.

(53) Sherrill, C. D. *J. Chem. Phys.* **2010**, *132*, 110902.

(54) Werner, H.-J.; Knowles, P. J. *J. Chem. Phys.* **1988**, *89*, 5803.

(55) Andersson, K.; Roos, B. O. In *Advanced Series in Physical Chemistry*; Yarkony, D. R., Ed.; World Scientific: Singapore, 1995; Vol. 2.

(56) Abrams, M. L.; Sherrill, C. D. *J. Phys. Chem. A* **2003**, *107*, 5611.

(57) Pierloot, K.; Dumez, B.; Widmark, P.-O.; Roos., B. O. *Theor. Chem. Acta* **1995**, *90*, 87.

(58) Gámez, J. A.; Serrano-Andrés, L.; Yáñez, M. *Phys. Chem. Chem. Phys.* **2010**, *5*, 1042.

(59) Veryazov, V.; Widmark, P.-O.; Serrano-Andrés, L.; Lindh, R.; Roos, B. O. *Int. J. Quantum Chem.* **2004**, *100*, 626.

(60) Sulzer, P.; Ptasinska, S.; Zappa, F.; Mielewska, B.; Milosavljevic, A. R.; Scheier, P.; Mark, T. D.; Bald, I.; Gohlke, S.; Huels, M. A.; Illenberger, E. *J. Chem. Phys.* **2006**, *125*, 044304.

(61) Papp, P.; Urban, J.; Matejcik, S.; Stano, M.; Ingolfsson, O. *J. Chem. Phys.* **2006**, *125*, 204301.

(62) Gámez, J. A.; Serrano-Andres, L.; Yáñez, M. *ChemPhysChem* **2010**, *11*, 2530.

(63) Gámez, J. A.; Serrano-Andrés, L.; Yáñéz, M. *Int. J. Quantum Chem.*, DOI: 10.1002/qua.23015.

(64) Roussyn, I.; Briviba, K.; Masumoto, H.; Sies, H. *Arch. Biochem. Biophys.* **1996**, *330*, 216.

(65) Briviba, K.; Roussyn, I.; Sharov, V. S.; Sies, H. *Biochem. J.* **1996**, *319*, 13.

(66) Chen, H.; Song, J. S.; Lai, W. Z.; Wu, W.; Shaik, S. *J. Chem. Theory Comput.* **2010**, *6*, 940.